Chapter 6
Mitral Valve

Liem Nguyen, MD and Neal Gerstein, MD

Abstract The mitral valve is a complex apparatus consisting of the annulus, leaflets, chordae tendineae, papillary muscle, myocardium, and its attendant chambers, the left atrium and ventricle. The function and competency of the mitral valve apparatus is intricately dependent on the structural integrity and coordination of each and all of its components. Structural or functional abnormalities contributing to mitral stenosis or mitral regurgitation and post-procedural changes can be evaluated with transesophageal echocardiography (TEE). With advancements in technology and the evolution of three-dimensional (3D) imaging, TEE is a necessary tool and modality for evaluating the mitral valve perioperatively.

Keywords Transesophageal echocardiography (TEE) · Mitral valve · Mitral regurgitation · Mitral stenosis · Proximal isovelocity surface area (PISA)

Anatomy and Function of the Mitral Valve Apparatus

The mitral valve apparatus consists of the annulus, leaflets, chordae tendineae, papillary muscle, myocardium, and its attendant chambers, the left atrium and ventricle (Fig. 6.1). Essentially, the entire left heart contributes to the function of

Electronic supplementary material The online version of this chapter (doi:10.1007/978-3-319-34124-8_6) contains supplementary material, which is available to authorized users.

L. Nguyen, MD (✉)
Department of Anesthesiology, University of California San Diego, 9300 Campus Point Drive #7651, San Diego, CA 92037-7651, USA
e-mail: liem@ucsd.edu

N. Gerstein, MD
Department of Anesthesiology, University of New Mexico, 2211 Lomas Blvd NE, Albuquerque, NM 87106, USA
e-mail: ngerstein@gmail.com

T.M. Maus et al. (eds.), *Essential Echocardiography*,
DOI 10.1007/978-3-319-34124-8_6

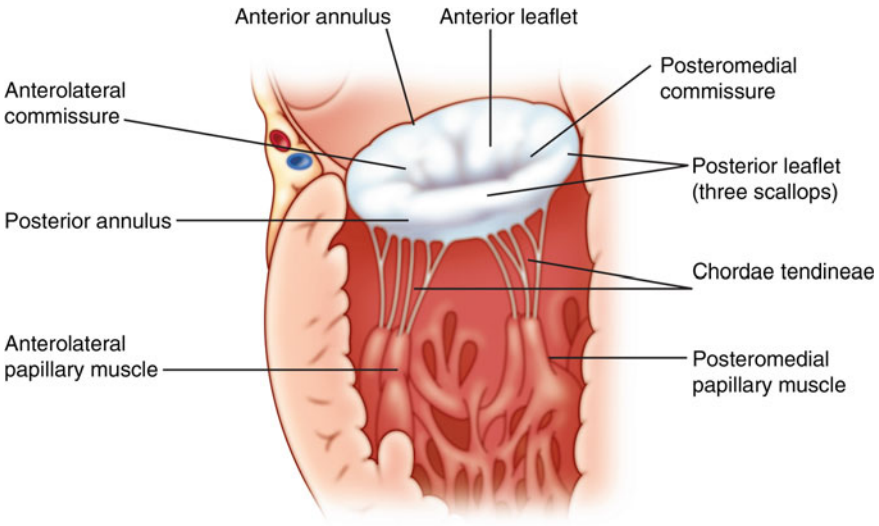

Fig. 6.1 Components of the mitral valve apparatus

the mitral valve. The function and competency of the mitral valve apparatus is intricately dependent on the structural integrity and coordination of each and all of its components [1–4].

The bicuspid mitral valve is composed of two anatomically distinct leaflets, the anterior and posterior leaflet. The anterior leaflet is located in close juxtaposition to the left and noncoronary cusps of the aortic valve, separated by a thin piece of tissue termed the aorto-mitral curtain. The posterior leaflet is unique in that it contains three identifiable subunits called scallops. In the commonly utilized Carpentier description of mitral valve anatomy, the scallops are labeled from anterior to posterior as P1, P2, and P3. While smaller in area than the anterior leaflet, the posterior leaflet subtends approximately two-thirds of the circumference of the annulus [1, 2, 4]. By contrast, the larger anterior leaflet in surface area only covers about one-third of the circumference of the annulus. The anterior leaflet is devoid of individual scallops, providing a smooth surface designed to promote systolic ejection of blood into the left ventricular outflow tract. Despite a lack of scallops, the Carpentier description notes segments A1, A2, and A3 which correspond to the posterior scallops (e.g., P1 coapts with A1, P2 coapts with A2, etc.) (Fig. 6.2). The anterior and posterior leaflets adjoin at two distinct points near the edges of the annulus (described below), which are termed the anterolateral and posteromedial commissures (Fig. 6.2) [2–4]. As an interdependent unit, the anterior and posterior leaflets come together and contact each other during systole to form a coaptation line resembling a semicircle (Figs. 6.2 and 6.3) [2, 3, 5]. The mitral leaflets are circumferentially supported by a fibrous-tissue reinforced ring structure referred to as the mitral annulus. The mitral annulus geometrically resembles a hyperbolic paraboloid or saddle shape, and anatomically serves as the attachment points for

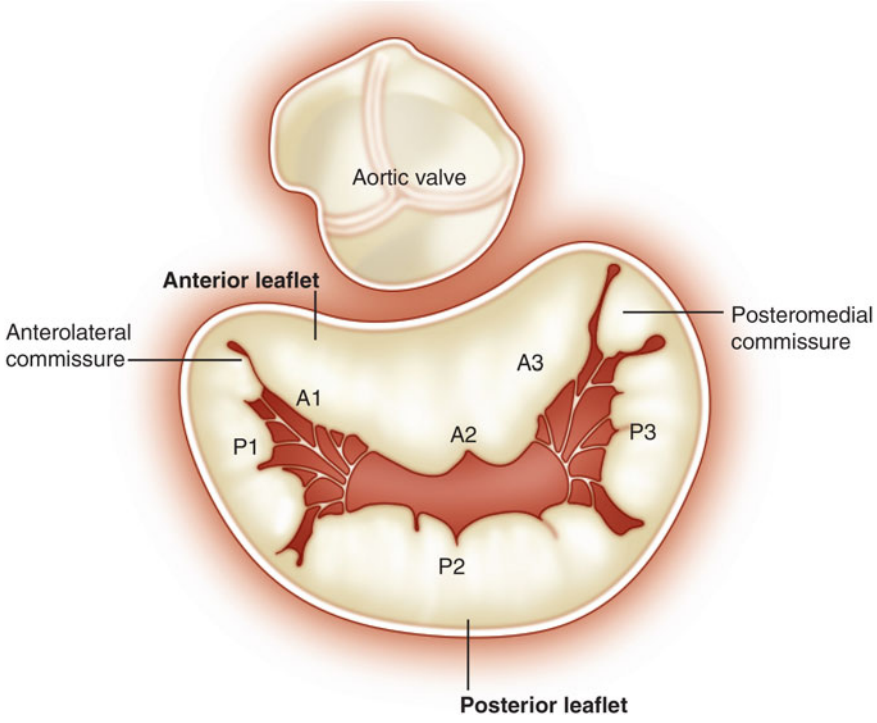

Fig. 6.2 Nomenclature of the bicuspid mitral valve according to the Carpentier classification

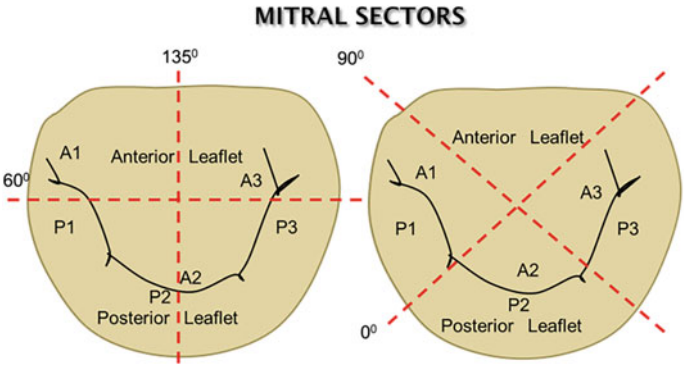

Fig. 6.3 Mitral sectors with representative leaflet segments expected from the midesophageal transesophageal views

both mitral leaflets. While a saddle has two high points (the front and back of a saddle) and two low points (the sides of the saddle), a mitral valve is similarly shaped with high and low points. The anterior–posterior (front to back) axis of the annulus defines the higher peak to peak dimension whereas the lateral axis (side to side or commissure to commissure) defines the trough to trough dimension, which is positioned at a lower point (Fig. 6.4a, b; Video 6.1). The posterior aspect of the mitral annulus is structurally thinner and contains less fibrous support, lending it to be more prone to dilation and flattening compared to the more reinforced anterior portion of the mitral annulus. Overall, the unique geometry of the saddle-shaped annulus serves to reduce the tension on both of the mitral leaflets during systole [5–9]. Underneath the mitral leaflets emerges a complex network of chordae tendineae that attach to both leaflets. The chordae tendineae are attached to the anterolateral and posteromedial papillary muscles and contract in concert to prevent the prolapse of the mitral leaflets into the atrium during systole [1, 4]. In summary, the coordinated movements of the mitral valve apparatus results in the closure of the mitral valve during systole and prevention of regurgitant flow into the left atrium.

TEE Imaging of the Mitral Valve

Assessment of the mitral valve begins with two-dimensional imaging of the entire mitral apparatus (Fig. 6.5a–f; Videos 2.1–2.3, 2.13, 2.15, and 2.16) [2, 3, 10, 11]. This can be performed by first starting in the midesophageal four-chamber view and obtaining multiplane images of all components of the mitral apparatus [2, 3, 10, 12]. The leaflet subunits of the mitral valve can be individually viewed as a two-dimensional slice using the available sector planes of the TEE probe at various multiplane angles (Figs. 6.3 and 6.5a–f). Instructions for how to obtain the various views discussed in this chapter can be found in Chap. 2.

Midesophageal Four-Chamber View (ME Four-Chamber View)

In the ME four-chamber view at 0° (Figs. 6.3 and 6.5a; Video 2.1), the anterior leaflet appears on the left side of the screen whereas the posterior leaflet is visualized on the right of the screen. The ME four-chamber view is useful for obtaining a global evaluation of bileaflet motion and the corresponding changes that may occur as a result of volume stress in the upstream atrium and downstream ventricle. The ME four-chamber is also useful to evaluate the degree of mitral regurgitation using color flow Doppler [2, 3, 10].

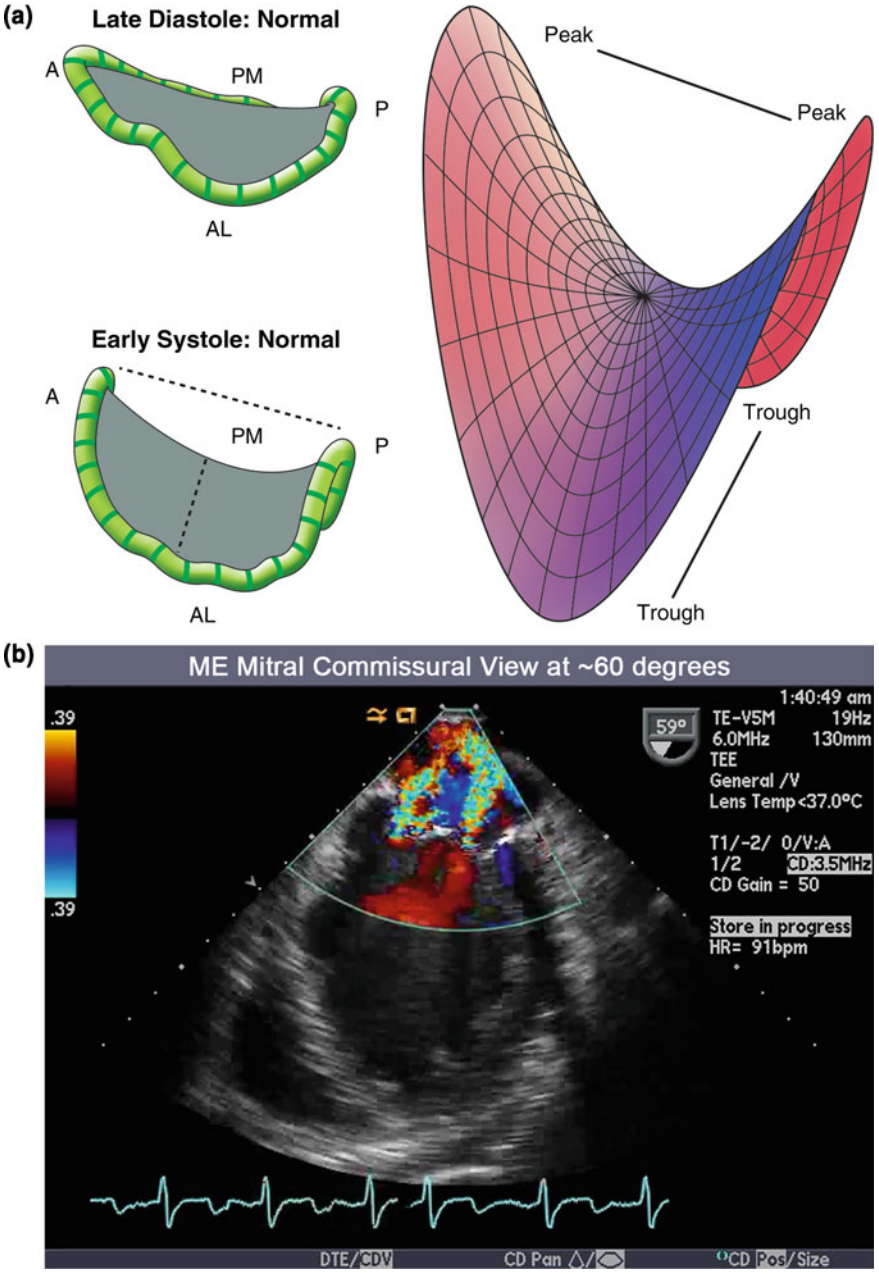

Fig. 6.4 **a** Rendition of mitral annulus depicting the characteristic saddle-shaped geometry. The *anterior–posterior axis* (ME LAX view) encompasses the peak to peak distance, whereas the *lateral axis* (ME mitral commissural view) corresponds to the trough to trough distance. **b** ME mitral commissural view with color flow Doppler demonstrating two distinct jets due to a sector plane that captures the two outer edges of the jet and omitting the central portion

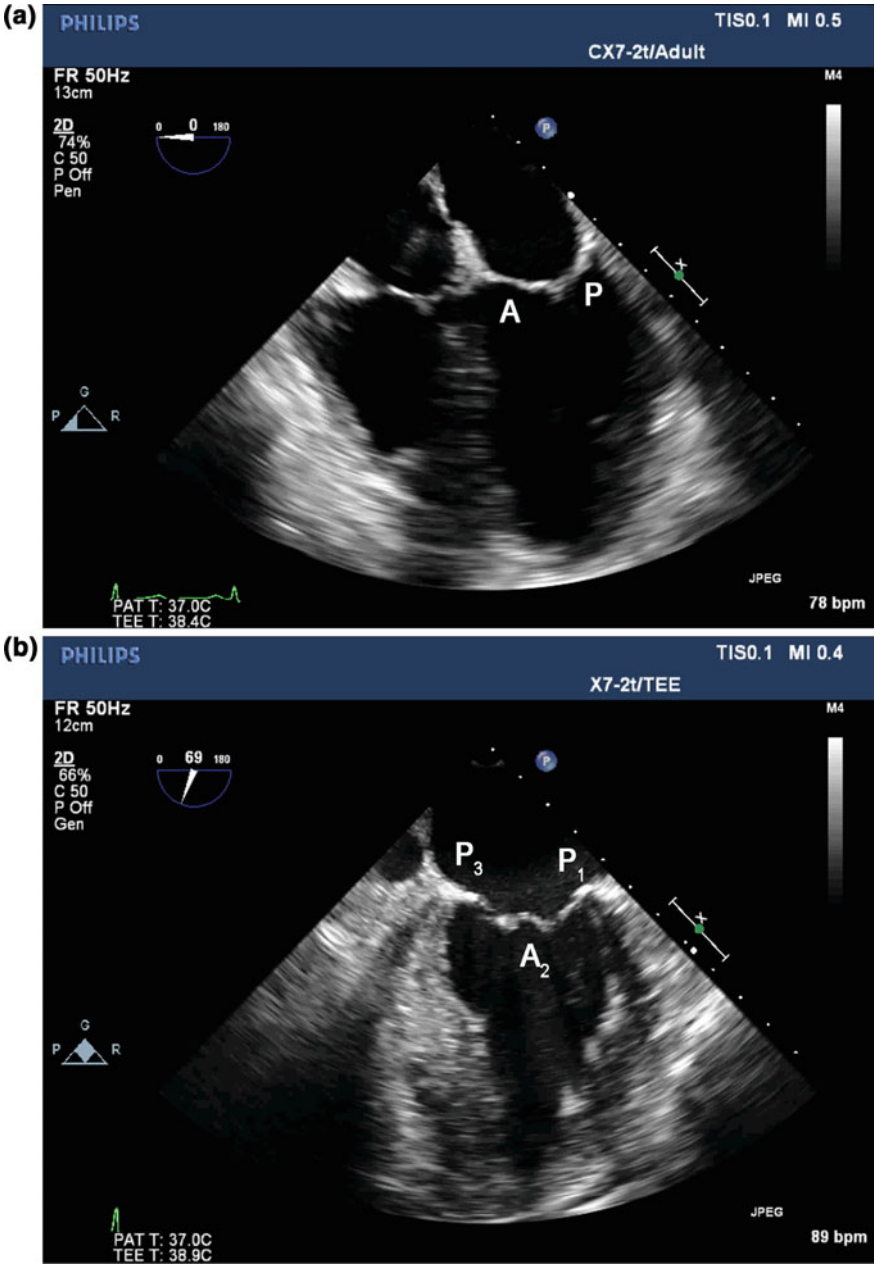

Fig. 6.5 TEE imaging of the mitral valve apparatus. **a** ME four-chamber view. **b** ME mitral commissural view. **c** ME two-chamber view. **d** ME LAX view. **e** TG basal SAX view. **f** TG two-chamber view. *A* anterior leaflet, *P* posterior leaflet

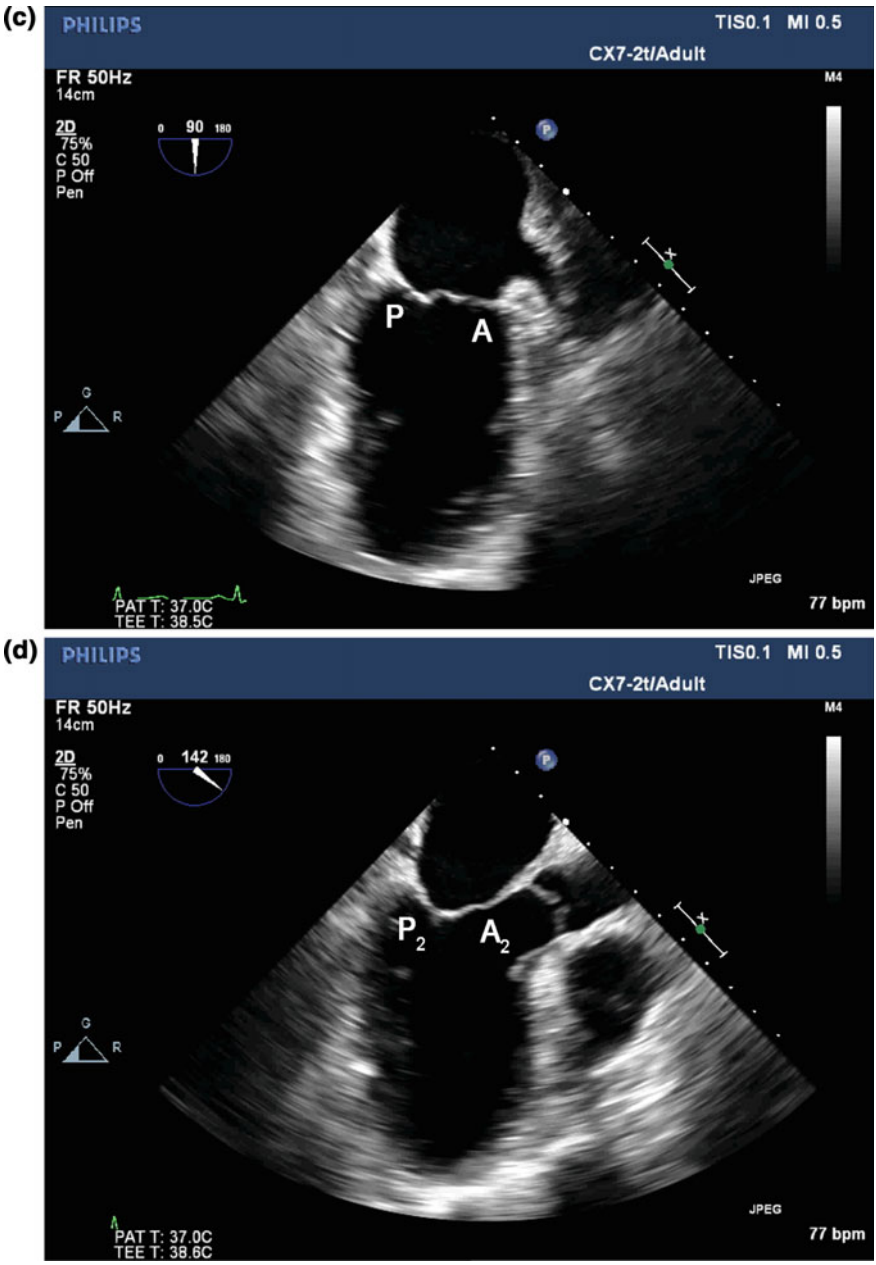

Fig. 6.5 (continued)

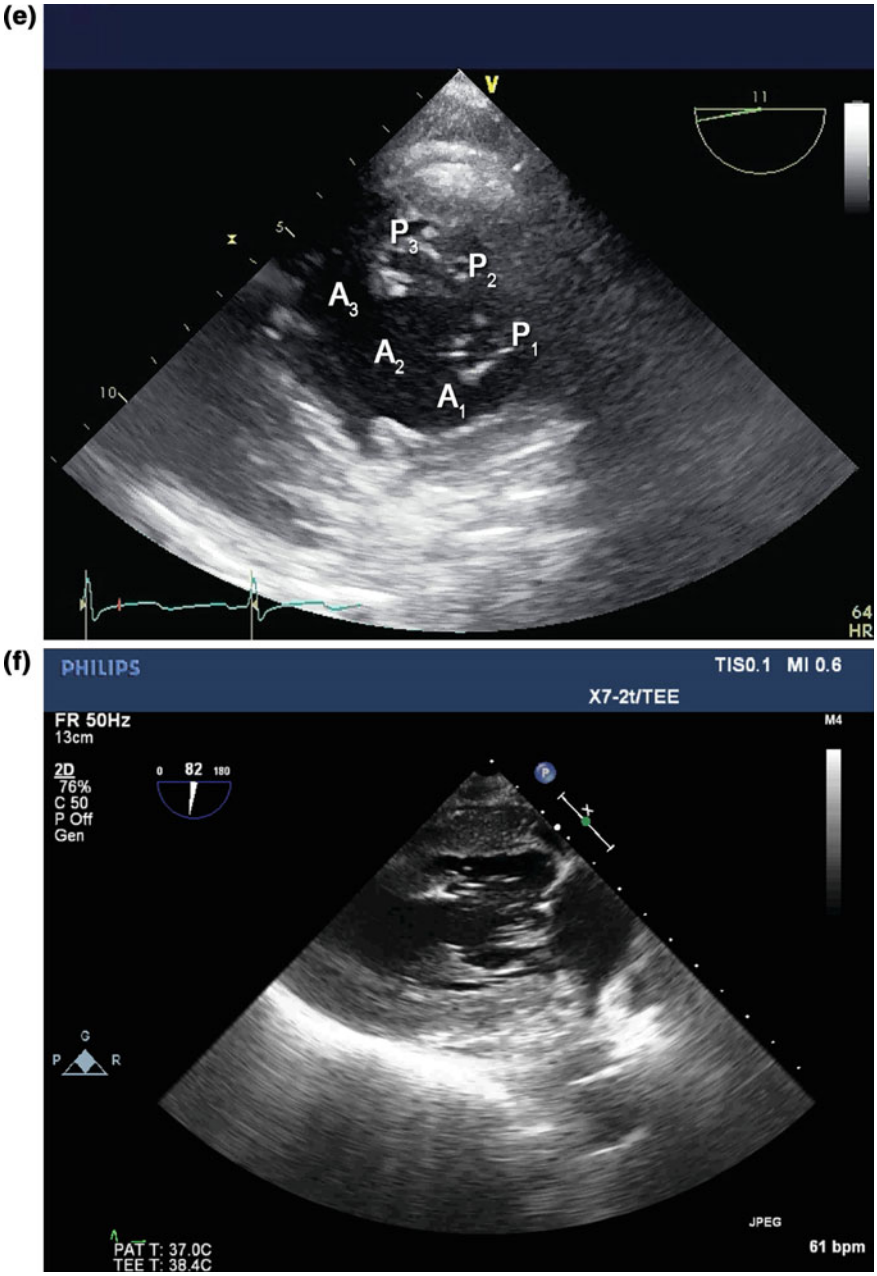

Fig. 6.5 (continued)

ME Mitral Commissural View

The ME mitral commissural view is obtained by starting at the ME four-chamber view and rotating the multiplane angle to approximately 45–60°. In this view of the mitral valve, the middle A2 segment is flanked by the P3 segment on the left and P1 segment on the right (Figs. 6.3 and 6.5b; Video 2.13) [2, 3, 10]. The ME mitral commissural view may also provide a view of the papillary muscles and their associated chordae tendineae. It is important to note that the ME mitral commissural view displays an imaging slice corresponding to a line that traverses the semicircle or curved coaptation point and the anterolateral and posteromedial commissures. Accordingly, Doppler color flow assessment of a regurgitant jet may appear as two distinct jets because the sector plane captures the two outer edges of the jet and omits the central portion (Fig. 6.4b; Video 6.1). This often results in the incorrect echocardiographic diagnosis of two distinct jets, when in fact the image merely represents the edges of one jet.

ME Two-Chamber View

The ME two-chamber view is obtained by rotating the multiplane angle to approximately 90° (Figs. 6.3 and 6.5c; Video 2.2). In this image plane, the anterior leaflet is positioned on the right and the posterior leaflet is on the left of the screen. The left atrial appendage and Coumadin ridge (a band of tissue separating the left atrial appendage and the left upper pulmonary vein) are often observed above and to the right of the anterior mitral leaflet. Withdrawing the probe from this position and turning slightly to the left often brings the left upper pulmonary vein into view, allowing for Doppler interrogation of left atrial inflow [2, 10].

ME Long-Axis View (ME LAX View)

The ME LAX view is obtained by increasing the multiplane angle to 120–140° until the aortic and mitral valve leaflets are seen opening and closing in the same image plane (Figs. 6.3 and 6.5d; Video 2.3) [2, 3, 10]. This imaging plane displays a slice of the mitral leaflets along the anterior–posterior dimension (A2–P2), perpendicular to the coaptation line. The A2 segment is displayed on the right of the screen nearest the aortic valve leaflets and the P2 segment appears on the left side of the screen. The ME LAX view allows for the echocardiographer to assess the anterior–posterior dimension of both the diameter of the mitral regurgitant jet and peak to peak distance of the mitral annulus (Fig. 6.4a). This view plane therefore offers a more accurate measurement of the width of the vena contracta, the narrowest part of a regurgitant jet at the level of the valve leaflets as measured by color flow Doppler, compared to other imaging planes [2, 3, 10].

Transgastric Basal Short-Axis View (TG Basal SAX)

The TG basal SAX view at 0° (Fig. 6.5e; Video 2.15) is obtained by either slightly withdrawing the probe or exerting anteflexion from the true transgastric midpapillary short-axis view of the left ventricle. The imaging plane is achieved when both the anterior and posterior mitral leaflets are visualized in a short axis, "fishmouth" view. The "fishmouth view" of the mitral valve allows for all the mitral segments to be viewed, providing a means to assess valve opening and closure from the left ventricular aspect. The TG basal SAX view may also reveal a ruptured chordae or flail segment from this vantage point. Moreover, color flow mapping of the regurgitant jet in the TG basal SAX view may reveal the origin of the coaptation defect and provide insight into the mechanism of regurgitation [3, 10].

TG Two-Chamber View

The TG two-chamber view at 90° (Fig. 6.5f; Video 2.16) provides a perpendicular scan plane that facilitates the assessment of the subvalvular apparatus (i.e., chordae tendineae and papillary muscle-LV wall complex) [10]. The anterolateral papillary muscle occupies a position furthest from the probe and the posteromedial papillary muscle is situated in the near field. This view is useful for evaluating the position and geometry of the papillary muscles, chordae tendineae and ventricular wall complex.

Mitral Regurgitation

Mitral regurgitation

2D	• Mitral leaflet motion (normal, excessive, restrictive) • Mitral calcification • Annular dimensions (dilated) • Left atrial enlargement, eccentric LV hypertrophy • LV wall motion abnormalities
CFD	• Qualitative assessment (Jet Area/LA Area ratio) • Coanda effect (wall hugging jet) • Vena contracta measurement
Spectral	• Pulmonary venous doppler (PWD) • Density of regurgitation jet profile (CWD) • PISA-based calculation of EROA

LV left ventricle, *LA* left atrium, *PWD* pulsed wave Doppler, *CWD* continuous wave Doppler, *PISA* proximal isovelocity surface area, *EROA* effective regurgitant orifice area

Although the final common pathway of an incompetent mitral apparatus is a regurgitant jet at the level of the leaflet tips due to a coaptation defect, a significant portion of MR is due to dysfunction of structures above and below the valve in the presence of normal leaflet motion [2, 3, 5, 13]. When considering the etiology or mechanism of MR, it may therefore be prudent to examine all the structures above and below the leaflets that comprise the mitral valve apparatus in order to fully characterize the mechanism. Furthermore, examination of leaflet motion according to Carpentier's classification can yield important clues into the mechanism of MR [2, 3]. The classification categorizes the mechanisms of MR into three types based upon the motion of the mitral valve leaflets: Type 1—normal leaflet motion; Type 2—excessive leaflet motion; Type 3—restricted leaflet motion. This categorization helps to organize the thought process around the types of MR as well as to help guide surgical therapy for the mitral valve.

MR associated with normal leaflet motion (Type 1) can be a result of mitral valve clefts, perforations, or most commonly annular dilation [2, 5]. The mitral annulus is reinforced by a network of fibroelastic tissue that serves to maintain the unique saddle-like geometry during systole (Fig. 6.4a) [5, 14–16]. Annular dilation, measured in the anterior–posterior dimension in the ME LAX view using caliper-based measurements, or distortion of the saddle-shaped geometry during systole may lead to a coaptation defect and represents an important mechanism of MR [6, 9, 16–20]. Left atrial enlargement (e.g., due to atrial fibrillation or ventricular dysfunction) and secondary annular dilation may contribute to MR in the setting of normal leaflet anatomy and motion. Dilation of the mitral annulus has also been implicated as a contributing etiology in ischemic MR [2, 3, 13, 19, 21, 22].

The ventricular myocardium, anterolateral and posteromedial papillary muscles, and network of chordae tendineae provide the strong foundation required for normal leaflet motion and competency (Fig. 6.1). The interpapillary distance (lateral distance) and location of the papillary muscles (i.e., apical displacement) in relation to the ventricular wall and coaptation point plays a significant role in the overall competency of the mitral valve complex [4, 5]. The major responsibility of the papillary muscle-chordae tendineae complex is to regulate leaflet movement. Excessive leaflet motion (Type 2), such as in the presence of a ruptured chord, results in leaflet prolapse and acute MR demonstrating that the papillary muscle and chordae tendineae work together to prevent leaflet displacement into the left atrium.

Abnormalities in leaflet anatomy such as seen in degenerative disease and endocarditis, may also result excessive leaflet motion, a coaptation defect and subsequent MR [2]. Degenerative mitral disease (i.e., Barlow's disease and fibroelastic deficiency) comprises a range of leaflet abnormalities characterized by chordal and leaflet thickening, mitral tissue redundancy, and excessive leaflet motion in the form of prolapse (Fig. 6.6a, b; Videos 6.2 and 6.3) or flail, leading to valve incompetency [5, 23]. Infective endocarditis and the presence of bacterial vegetations on the atrial side often causes leaflet damage, leading to marked destruction of both the anatomy and function of the leaflets (Fig. 6.6c, d; Videos 6.4 and 6.5). Extensive damage may result in excessive leaflet motion and be classified

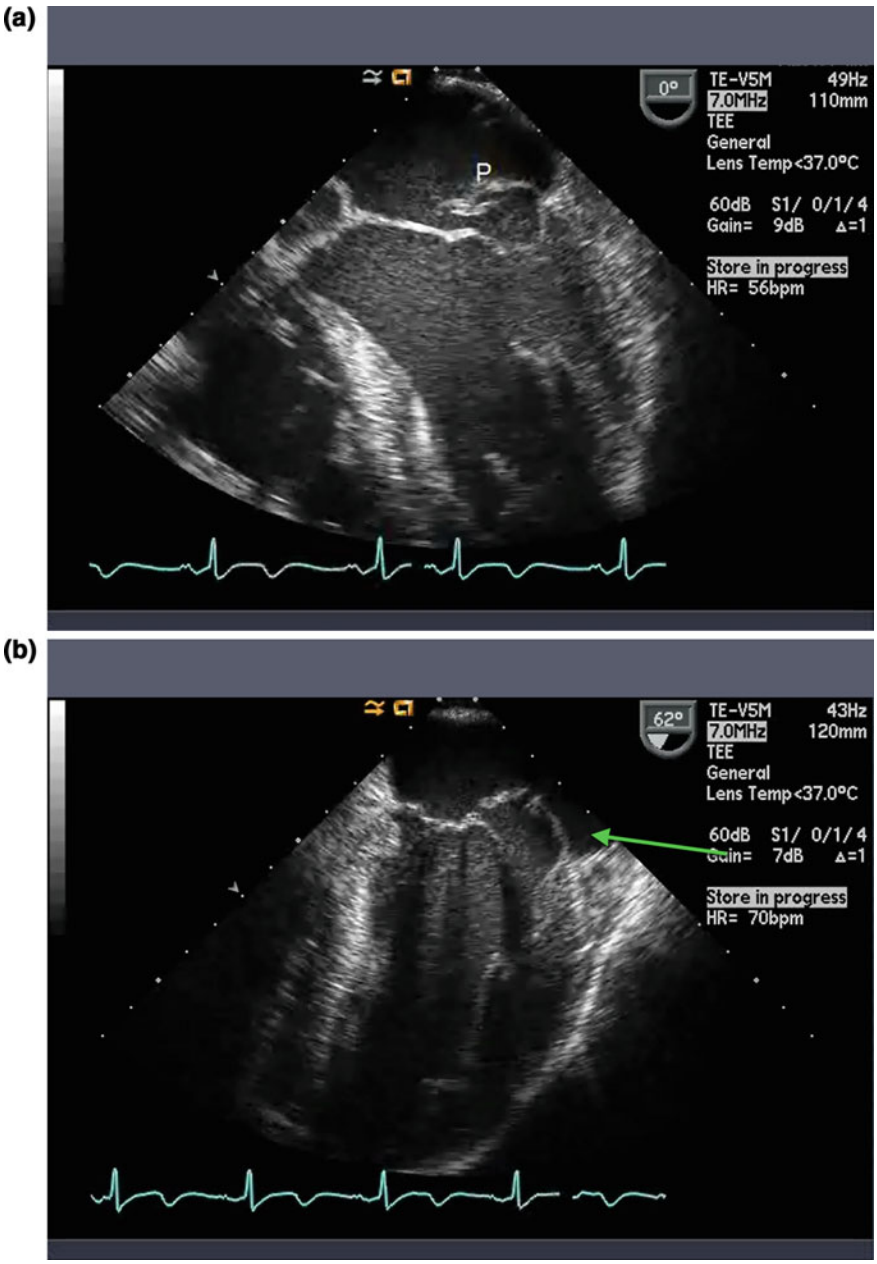

Fig. 6.6 **a** ME four-chamber view with posterior leaflet prolapse (P). **b** ME mitral commissural view of the same patient with posterior leaflet prolapse (*green arrow*). **c** ME four-chamber view with anterior leaflet vegetation (*red arrow*). **d** ME LAX view of the same patient with an anterior leaflet vegetation (*red arrow*)

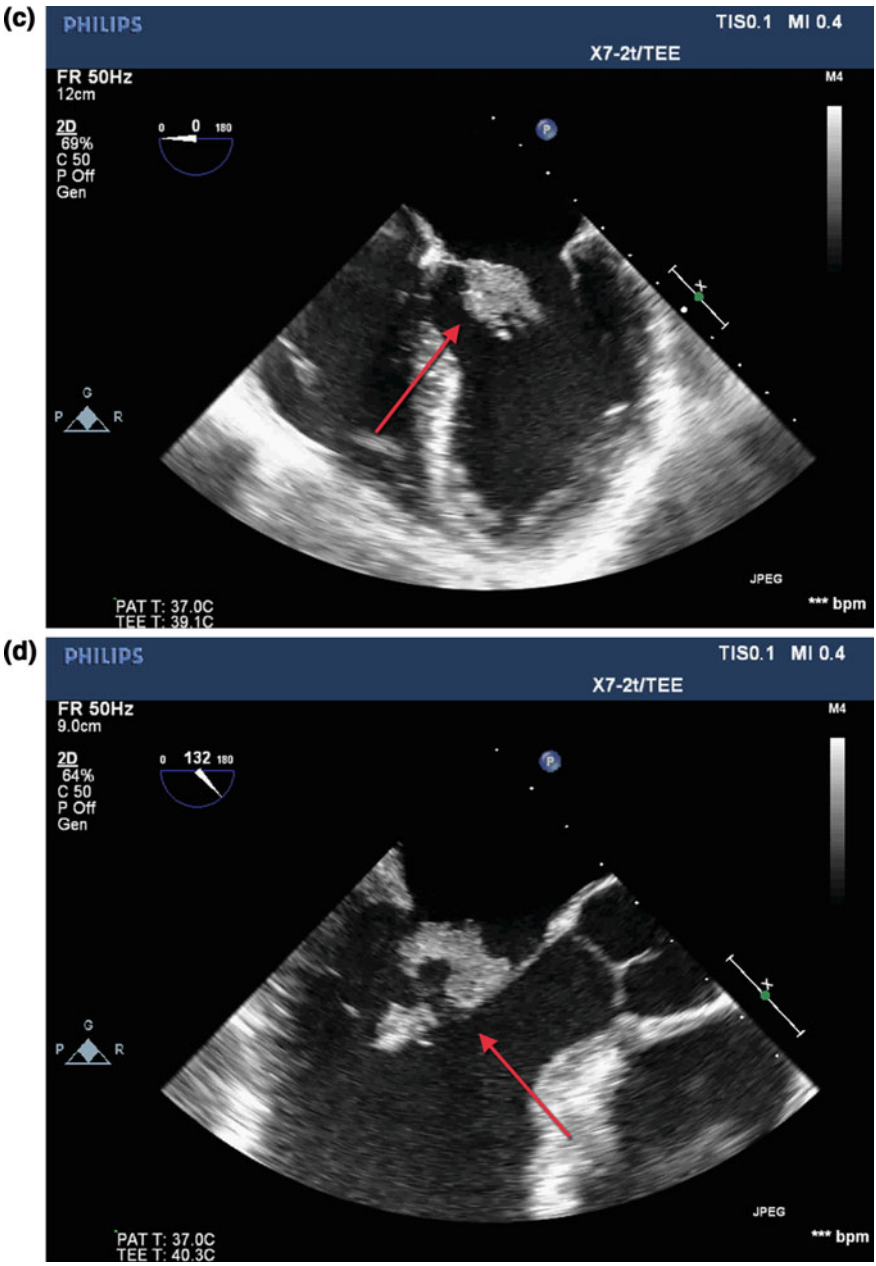

Fig. 6.6 (continued)

as Type 2 MR, while healed endocarditis may have a resultant perforation in a leaflet but otherwise normal leaflet motion and be classified as Type 1.

Restriction of the mitral valve leaflet motion is classified as Type 3 and may be subdivided based upon the restriction in systole and diastole (Type 3a) and during systole only (Type 3b). Leaflet calcification and fusion as seen in rheumatic disease (Type 3a) is an underappreciated etiology of MR where leaflet motion is impaired in systole and diastole. In addition to marked leaflet immobility, the annulus and entire subvalvular apparatus may also deteriorate from marked calcification.

Patients with functional mitral regurgitation (FMR) (Type 3b) underscore the critical geometrical relationship of the ventricular wall, papillary muscle, and chordal elements in providing a strong foundation for normal leaflet coaptation. The term "functional mitral regurgitation" refers to the dysfunction of the left ventricle as the underlying cause of MR in the setting of normal leaflet anatomy. Most commonly, FMR is a result of myocardial ischemia or dilated cardiomyopathy with distortion of the normal geometry of the ventricular myocardium, papillary muscles, and chordae network. Indeed, the proper interpapillary distance (lateral distance) and location of the papillary muscles (i.e., apical displacement) in relation to the ventricular wall and coaptation point is critical in regulating the overall competency of the mitral valve complex [4]. In the setting of myocardial ischemia, displacement of the papillary muscles toward the apex of the heart and concomitant tethering of attached chordae culminates in leaflet restriction and formation of a coaptation defect [13, 21].

In summary, the closing forces of the mitral apparatus are dependent on the intricate relationship of the leaflets, annulus, chordae tendineae, papillary muscles, atrial, and ventricular myocardium. Disruption of any component in the chain may result in mitral incompetency.

Grading Severity (Table 6.1)

Two-dimensional Echocardiography

Prior to quantifying the severity of MR, it may be prudent to examine the upstream and downstream chambers (left atrium and left ventricle, respectively) for signs of adaptation to volume stress. Adaptation to chronic volume overload may lead to

Table 6.1 Mitral valve regurgitation quantitative assessment

	Mild	Moderate	Severe
Vena contracta (mm)	<3	3–7	**>7**
Pulmonary venous Doppler	Normal	S wave blunted	**S wave reversal**
EROA by PISA (cm^2)	<0.20	0.20–0.40	**>0.40**

Criteria for severe MR is highlighted in bold

chamber dilation of the left atrium and left ventricle, which may be appreciated on two-dimensional imaging [5, 10]. Upstream effects of left atrial volume overload and pulmonary hypertension may result in echocardiographic signs of right ventricular (RV) dilation, tricuspid regurgitation, and septal bowing suggestive of RV dysfunction. Echocardiographic signs of the downstream effects of MR may include the presence of eccentric LV hypertrophy, elevated end diastolic volumes, and increased (presence of ventricular dysfunction) or decreased (supranormal ejection fraction in compensated chronic MR) end systolic dimensions. After examining the chambers of the heart for the effects of volume overload, specific attention can then be afforded to the rest of the mitral apparatus.

While two-dimensional echocardiography does not directly allow gradation of severity of MR, it certainly alludes to a mechanism for the MR. Observation of a significant coaptation defect (lack of anterior and posterior leaflets coming together in systole) suggests that MR will exist. The cause of the coaptation defect may be categorized under one of the three types of leaflet motion described above. Evidence of excessive leaflet motion (Type 2) is generally a result of degenerative disease of the mitral valve leading to prolapse, flail, or billowing of a leaflet segment above the annular plane [2, 23]. More specifically, prolapse is defined as a translation of the leaflet tip above the annulus due to excess leaflet and/or chordal length during systole (Figs. 6.6a, b and 6.7; Video 6.6). The term flail refers to the movement of leaflet tip above the annular plane as a result of a ruptured chordae. The presence of a ruptured chordae may often be obscured, rendering the echocardiographic distinction between prolapse and flail challenging. Billowing or scalloping is a projection of leaflet body or segment (not leaflet tip as in prolapse) above the annulus with the point of coaptation remaining below the annular plane [5, 23]. MR as a result of excessive motion of an isolated leaflet often results in an eccentric jet directed away from the diseased leaflet as it emerges through the coaptation defect (Fig. 6.7). Although uncommon, eccentric jets may be present in bileaflet disease if one of the leaflets is more affected than the other. Nevertheless, the appearance of an eccentric jet often signifies the presence of a structural abnormality in the mitral apparatus and thus warrants close examination.

Restricted leaflet motion in systole and diastole (Type 3a) is associated with rheumatic disease [24]. This differs from functional MR (Type 3b) in which restricted leaflet motion is only in systole due to leaflet tethering as a result of a dilated ventricle or papillary muscle ischemia. The direction of the jet often emerges toward the affected leaflet if the restricted leaflet motion is asymmetric. In the case of symmetric bileaflet tethering, a central jet may result [2, 3].

Color Flow Doppler

Color flow Doppler enables the echocardiographer to initially screen and map the mitral regurgitant jet as it occupies the left atrium (Fig. 6.8a–d; Videos 6.7–6.10) [3, 10]. To optimize the image quality, it may help to utilize the zoom function to increase the window size of the chamber of interest. With a Doppler flow sector

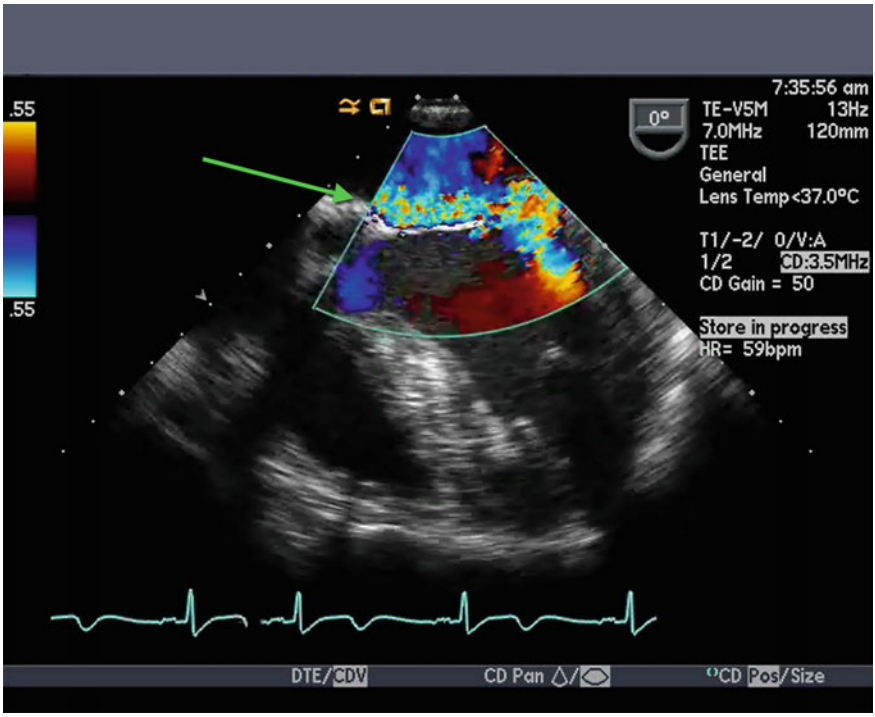

Fig. 6.7 ME four-chamber view with CFD in the patient from Fig. 6.6. Posterior leaflet prolapse with corresponding jet directed away from affected leaflet

window set to capture only the left atrium, mapping of the MR jet can then be optimized by setting the Nyquist limit (the maximum detectable velocity of the Color Map Scale, see Chap. 3) to approximately 50–70 cm/s. It may be prudent to visualize the jet in multiple views to gain a complete picture of the nature and contour of the regurgitant volume. In this way, jets that are difficult to visualize (e.g. wall hugging or eccentric jets) are not missed or underappreciated. It may also be helpful to make small adjustments to the probe position to maximize the quality of the image and capture the most representative jet possible. This may require slight anteflexion/retroflexion, advancement/withdrawal, or leftward/rightward turn of the probe while imaging the MR jet with color flow Doppler. Once the MR jet is fully imaged, it is important to make a qualitative assessment of the regurgitant flow focusing on the jet shape, direction, width, area, presence of eccentricity, and distance traveled into the left atrium. Color flow Doppler examination of the MR jet is an important first step to obtaining an initial impression and grading the severity of regurgitation [3, 5].

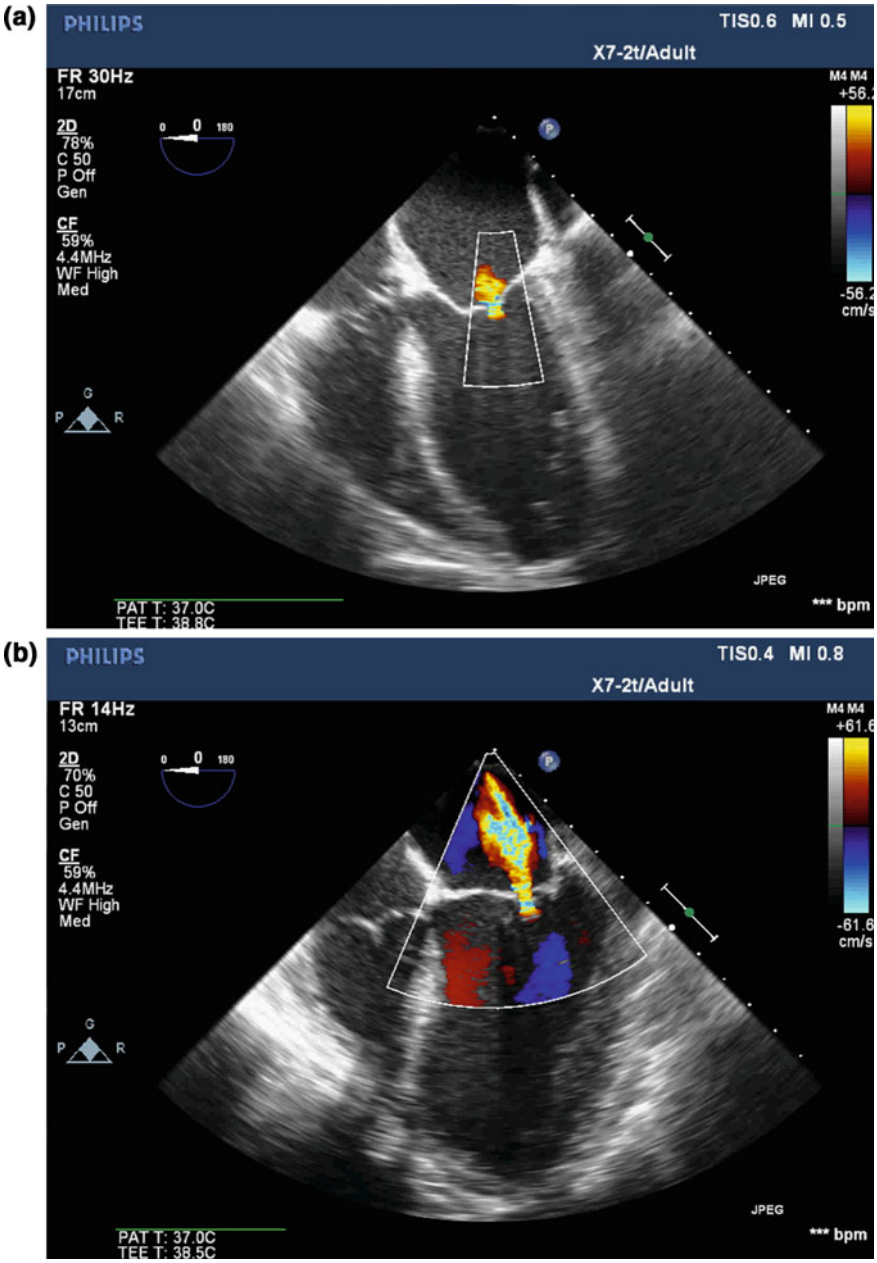

Fig. 6.8 Color flow Doppler showing increasing MR severity. **a** Trace MR (1+), **b** mild MR (2+), **c** moderate MR (3+), **d** severe MR (4+)

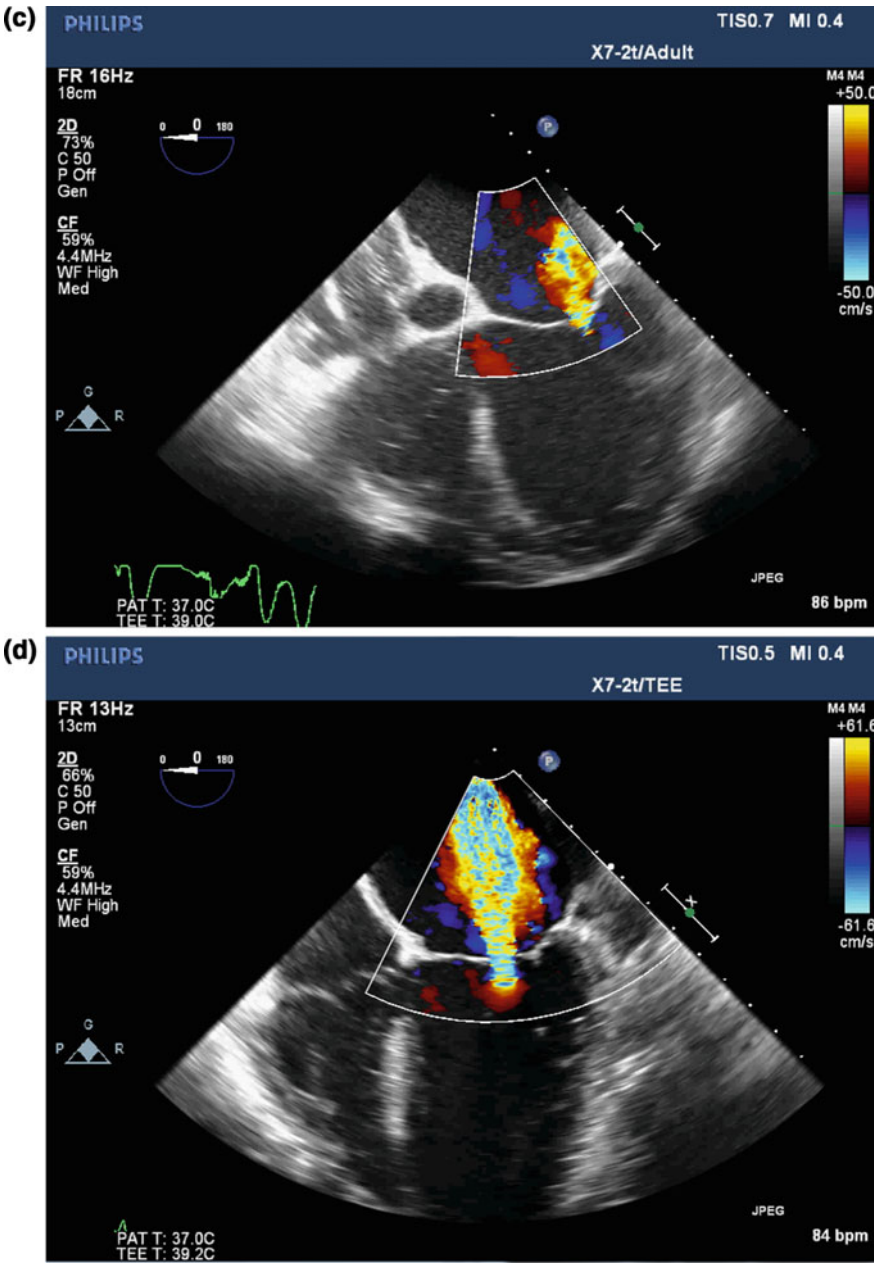

Fig. 6.8 (continued)

Vena Contracta

Measurement of vena contracta (Fig. 6.9a) is a quick and useful method to assess the severity of mitral regurgitation [3, 5, 25, 26]. The vena contracta is the narrowest part of the regurgitant jet visualized with color flow Doppler as it emerges from the regurgitant orifice at the level of the leaflet tips [2, 3]. The ideal image captures a jet profile that consists of a proximal convergence zone (area of flow acceleration on ventricular side) and a narrow neck at the plane of the coaptation point. The vena contracta measurement is advantageous as it is relatively independent of machine settings and loading conditions [5]. However, precise measurement of the vena contracta width can often be challenging due to difficulties in proper image acquisition and the small dimensions of the jet width. The image of the jet can be optimized using the zoom function and setting the Nyquist limit to approximately 50–70 cm/s. The ideal acoustic window to capture the anterior–posterior dimensions (perpendicular to coaptation point) of the regurgitant jet corresponds to the ME LAX view (at ~120–150°). It may be necessary to fine-tune the image by turning the probe leftward or rightward to obtain an optimal jet profile. If a jet is not visualized in the ME LAX view, the vena contracta can also be measured in the ME four-chamber view, but this measurement should be interpreted with caution as it does not measure the jet perpendicular to the coaptation line. It may be helpful to take several measurements to obtain a more precise vena contracta measurement. Vena contracta measurements above 7 mm constitute severe MR and values below 3 mm constitute mild MR [2, 5].

Pulmonary Venous Flow Profile

Doppler interrogation of the pulmonary venous flow or left atrial inflow (Fig. 6.9b) can be used as a semi-quantitative method for grading MR severity [2, 3, 10, 26]. Using pulse wave Doppler, a sample volume of left atrial inflow can be captured, usually using the left upper pulmonary vein. With the point of interrogation cursor set approximately 1 cm into the pulmonary vein, velocities are measured as flow moves into the left atrium. The speed or velocity of blood flow traveling towards the left atrium during systole is typically greater than the speed during diastole, yielding a systolic dominant pulmonary venous pattern ($\text{Systolic}_{\text{velocity}} > \text{Diastolic}_{\text{velocity}}$ or $S/D > 1$).

The presence of systolic mitral regurgitation may reduce the peak systolic velocity of the pulmonary venous flow as the regurgitant jet accelerates back through the atrium and into the pulmonary venous bed. As the regurgitant jet flows into the pulmonary veins and meets the incoming left atrial flow during systole, blunting ($S_{\text{velocity}} < D_{\text{velocity}}$ or $S/D < 1$, Fig. 6.9b) or reversal (below baseline) of the systolic component of the pulmonary Doppler profile is observed. Systolic reversal of flow in the pulmonary venous profile is a specific but not sensitive

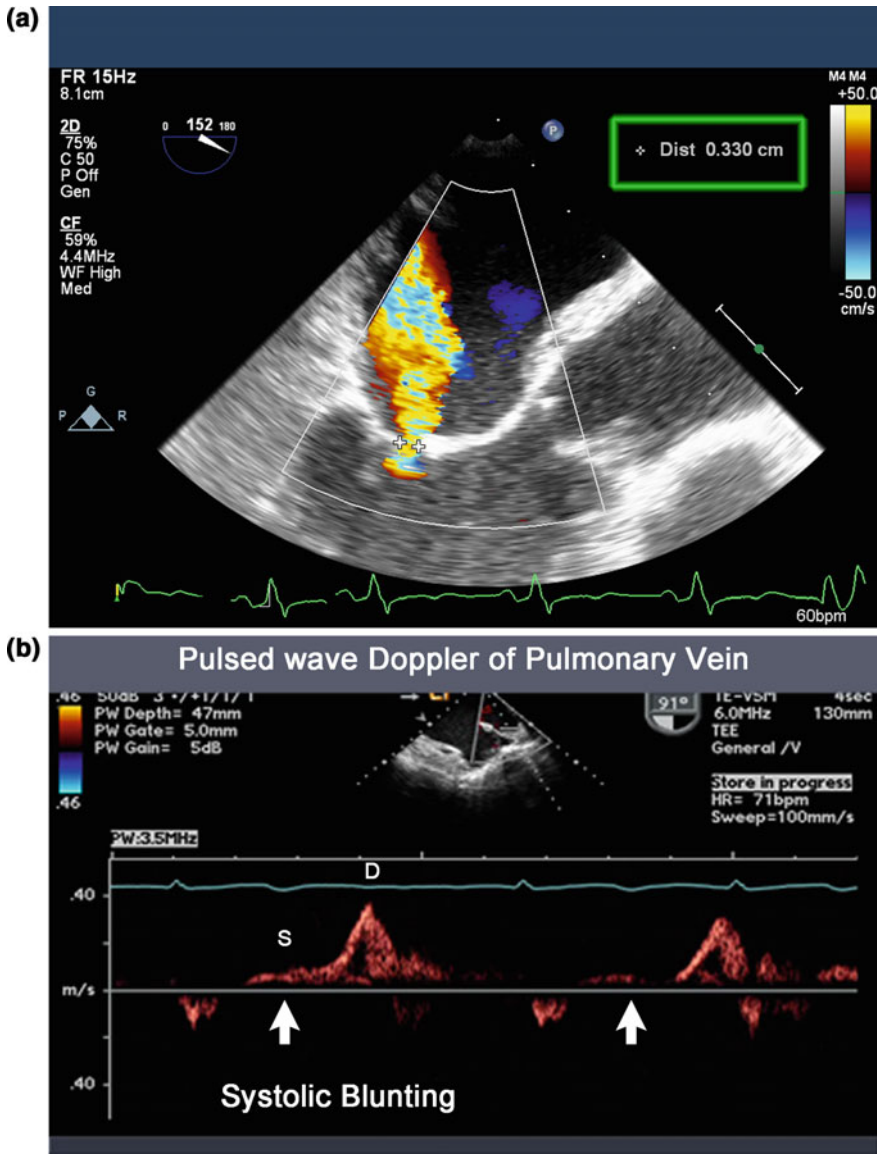

Fig. 6.9 **a** Vena contracta measurement. Notice that the measurement is taken at the narrowest portion or neck of the jet as it crosses the plane of coaptation. **b** Pulse wave Doppler interrogation of pulmonary veins demonstrating systolic blunting in a patient with moderate MR

finding of severe MR, with systolic blunting representing a more moderate degree of MR [5]. The poor sensitivity of the pulmonary venous flow in detecting MR is partly due to the varying degrees of left atrial compliance in certain patients and the challenge of interrogating all four pulmonary veins on TEE [2, 3].

Proximal Isovelocity Surface Area (PISA)

The proximal isovelocity surface area (PISA) method is a quantitative modality for grading MR (Fig. 6.10) [26–28]. The PISA method is an application of the continuity equation and provides a means to calculate the effective regurgitant orifice area (EROA). In simple terms, the volume or flow of blood below the mitral valve is equal to the volume or flow of blood above the mitral valve. As a regurgitant jet travels towards the narrowed mitral orifice, the column of blood accelerates and a series of concentric hemispheres are generated on the ventricular side of the mitral valve. When blood velocity increases beyond the limit of detection of the Doppler (i.e., Nyquist limit), the color flow map near the mitral orifice displays a high velocity region with evidence of aliasing (blood velocities above the limit of detection appear to reverse). Volume or flow of blood in the convergence zone (ventricular side) is equal to the product of the surface area of the first hemisphere or isovelocity shell and its associated aliasing velocity $\left(\text{Flow} = 2\pi r^2 \times V_{\text{aliasing}}\right)$. The radius ($r$) of the isovelocity shell is defined by the distance from the regurgitant orifice to the border of the first aliasing velocity. Volume or flow on the atrial side is calculated as the product of the effective regurgitant orifice area (EROA) and peak

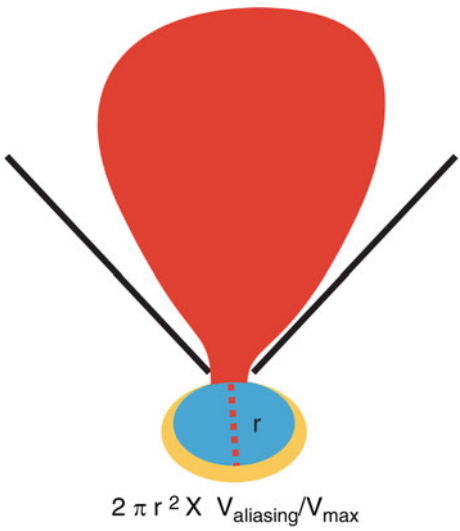

Fig. 6.10 Calculation of the effective regurgitant orifice area of MR by PISA

velocity of the MR jet ($V_{\text{MR Jet}}$). For this calculation, the peak velocity of the MR jet is measured using continuous wave Doppler interrogation along or parallel to the regurgitant flow.

Applying the continuity principle of equal flow on the atrial and ventricular side of the regurgitant orifice, the EROA can be calculated as follows:

$$\text{EROA} = 2\pi r^2 \times V_{\text{aliasing}} / V_{\text{MR jet}}$$

r = radius of the first isovelocity shell; V_{aliasing} = Nyquist limit; $V_{\text{MR jet}}$ is the peak velocity of the MR jet and $\pi = 3.14$.

The PISA method allows for calculation of the EROA and represents a true quantitative measurement of MR severity. An EROA >0.4 cm^2 corresponds to severe MR while an EROA <0.2 cm^2 corresponds to mild MR. It is important to highlight that the PISA method is fraught with several limitations. The PISA calculation requires several steps and is based on meticulous measurements of small dimensions, rendering this technique time-consuming and laborious for clinical application in the operating room. The shape of the isovelocity shells are also assumed to be hemispheres when indeed they may not be. Nevertheless, the PISA method may prove useful in cases where quantitative analysis is necessary to distinguish between moderate MR from mild or severe forms [27, 28].

Hemodynamics

The MR jet is one of the most dynamic and load dependent lesions owing to the large pressure gradient between the LV and LA during systole. The degree of MR at any point in time is extremely sensitive to hemodynamics with numerous studies demonstrating the dynamic nature of MR under different loading conditions. The degree of MR has been shown to decrease with the reduction of preload and afterload that is associated induction of general anesthesia. By contrast, increasing afterload with phenylephrine and preload augmentation with fluid administration has been shown to provoke or worsen the MR jet under general anesthesia. The effects of general anesthesia often poses a challenge for the intraoperative echocardiographer as the preoperative awake hemodynamics may significantly differ from that found in the operating room. It may prove useful to make note of the precise hemodynamic state of the patient at the time of intraoperative echocardiographic assessment and compare the parameters to the baseline or preoperative loading conditions [5].

Mitral Stenosis

Mitral Stenosis

2D	• Mitral leaflet motion (restrictive) • Mitral annular and leaflet calcification • Left atrial enlargement • LA spontaneous echo contrast (LAA thrombus identification) • Small LV dimensions (underfilled) • Planimetry
CFD	• Flow acceleration on left atrial aspect • Turbulent flow entering LV
Spectral	• PHT–CWD • Mean gradient–CWD • MVA–PHT-based calculation, PISA-based calculation

LA left atrium, *LV* left ventricle, *LAA* left atrial appendage, *PHT* pressure half time, *CWD* continuous wave Doppler, *MVA* mitral valve area, *PISA* proximal isovelocity surface area

The mitral valve (MV) assumes its largest area during diastole as it serves as a conduit for left ventricular filling. The normal mitral valve area is approximately 4–6 cm^2, with significant elevations in the gradient across the MV as the area approaches 1.0 cm^2. Upstream from the stenotic mitral valve, a marked increase in left atrial pressure is observed followed by chamber enlargement, stagnant blood flow, and atrial dysrhythmias. As the disease process progresses, marked elevations in left atrial pressure and pulmonary hypertension can precipitate right heart dysfunction. As blood converges near the narrow orifice, flow accelerates across the valve as it enters the left ventricle. Downstream from the MV stenosis, an LV with lower end diastolic volume from restricted filling is often evident on two-dimensional echo [3, 24, 29].

Two-dimensional Echocardiography

Mitral stenosis (MS) is the result of a reduction in the valve area during diastole from impaired valve opening. Although rheumatic heart disease is commonly associated with mitral stenosis, nonrheumatic causes of MS have recently become more important causes of MS [2, 24]. Nonrheumatic causes of mitral stenosis include severe leaflet and annular calcification, congenital mitral defects like parachute deformity (in which all chordae originate from a single papillary muscle), infective endocarditis, LA thrombus or myxoma, carcinoid syndrome, and post-repair or valve replacement associated MS [24]. The anatomic changes

associated with the above-mentioned processes are often discernible on two-dimensional echocardiography. Besides appreciating a reduction in valve opening in the TG basal SAX view and ME views, echocardiographic signs of calcific MS may include evidence of leaflet thickening, echogenic calcification, retraction or shortening, fusion of the commissures and leaflet immobility. Two-dimensional echocardiography often reveals calcium deposition extending to the subvalvular apparatus and mitral annulus, which may be visualized in the ME mitral commissural and TG LAX views.

In the case of rheumatic MS, the characteristic doming of the anterior leaflet or formation of a "hockey stick" like appearance may be appreciated in the ME four chamber and ME LAX views (Fig. 6.11; Video 6.11). The unique pattern of calcification beginning at the leaflet tips renders this portion relatively immobile compared to the remaining mobile midportion or body. By contrast, calcific MS usually starts near the annulus and extends into the leaflets near the base and usually does not involve the commissures or leaflet tips until later in the disease process. Two-dimensional examination of the upstream effects of MS may reveal signs of adaptation to LV inflow obstruction. Upstream echocardiographic signs of chronic MS may include the presence of spontaneous echo contrast or early thrombus formation, marked LA enlargement, systolic blunting of the pulmonary venous flow, concomitant MR, RV dysfunction with paradoxical septal motion, RA enlargement with bulging of the interatrial septum, and tricuspid regurgitation. Just

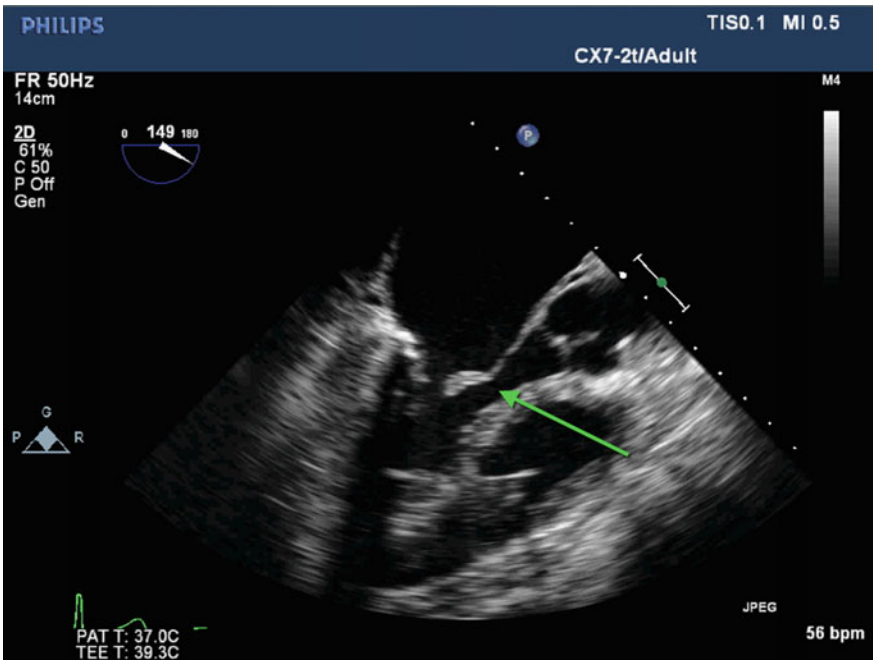

Fig. 6.11 "Hockey stick" deformity (*green arrow*) in a patient with rheumatic mitral stenosis

Table 6.2 Mitral valve stenosis: quantitative assessment

	Mild	Moderate	Severe
PHT (ms)	100	200	**>220**
Mean gradient (mmHg)	6	6–10	**>10**
Valve area[a] (cm^2)	1.6–2.0	1.0–1.5	**<1.0**

Criteria for severe MS is highlighted in bold
PHT Pressure half time
[a]Valve area as determined by PHT formula, PISA calculation or planimetry

proximal to the stenotic mitral valve, an area of flow convergence is observed on color flow Doppler as blood accelerates into the narrow orifice. As blood crosses the plane of the valve, a population of high aliasing velocities beyond the limit of detection (Nyquist limit) emerge and are displayed as a region of turbulent flow on the color Doppler map.

Quantitative Assessment of Mitral Stenosis

The following sections describe the different quantitative echocardiographic assessments of mitral stenosis (Table 6.2).

Pressure Gradients

As the underlying cause of mitral stenosis progresses, an increase in the LA–LV transvalvular gradient develops as flow accelerates across the narrow opening. The pressure differential (ΔP) between the LA and LV is described by the modified Bernoulli's equation or $\Delta P = 4v^2$, where v is the instantaneous peak velocity of blood across the valve and ΔP is the pressure difference or gradient. The ME four chamber and ME LAX views can be used measure the transvalvular gradient across the mitral valve. Using continuous wave Doppler interrogation, it is important to align the sampling cursor parallel to the direction of LV inflow. The resultant transmitral inflow profile and velocity time integral (VTI) describes the observed increase in velocities across the valve and delayed time for the LA and LV pressures to reach equilibrium due to the stenotic orifice. From the transmitral inflow profile, a mean gradient can be determined by tracing the area under the early filling (E-wave) and late filling (A-wave) waves in their entirety (Figs. 6.12 and 6.13a, b). The peak gradient or velocity describes the greatest pressure differential or velocity of the fastest red blood cell of the entire population. More importantly, the mean gradient is a value that represents the average pressure difference or velocity of the entire column of blood moving from the atrium to the ventricle across the stenotic orifice. The mean gradient derived from the VTI or area under the curve is used in grading severity of mitral stenosis [24].

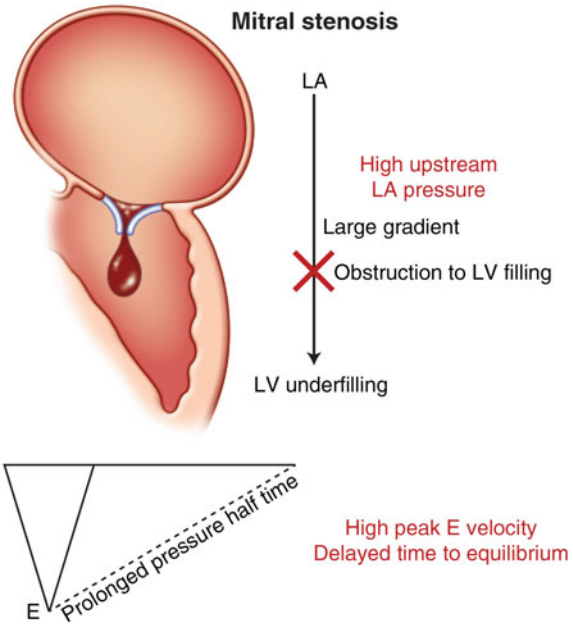

Fig. 6.12 Flow dynamics of mitral stenosis resulting in an elevated peak E-wave velocity and prolonged pressure half time downstream from stenotic orifice

Mitral Valve Area Calculations

Pressure Half Time (PHT)

As blood moves across the stenotic mitral valve, the pressure gradient between the left atrium and ventricle begins to dissipate proportional to the degree of stenosis. Similarly, the maximum peak instantaneous velocity of blood decelerates over time proportional to the severity of MS. The more severe the obstruction to flow, the longer it takes for the pressure in the LA and LV to equilibrate (Fig. 6.12). The pressure half time (PHT) describes the slope or rate at which the atrial and ventricular pressure differential decreases by 50 %. The more severe the stenosis, the longer it takes for the LA and LV pressures to equalize and thus, a more prolonged PHT (Figs. 6.12 and 6.13a, b). A PHT measurement as long as 300 ms corresponds to severe MS whereas a normal mitral valve area with an insignificant transvalvular pressure difference exhibits a PHT of ~50 ms. The PHT is inversely proportional to the mitral valve area (MVA) and is defined by the equation

$$\mathrm{MVA}(\mathrm{cm}^2) = 220/\mathrm{PHT}\ (\mathrm{milliseconds})$$

In the ME four chamber or ME LAX view, the PHT is obtained by aligning the Doppler beam parallel to the direction of flow through the MV and using continuous wave Doppler to interrogate LV inflow. The PHT is then measured by taking

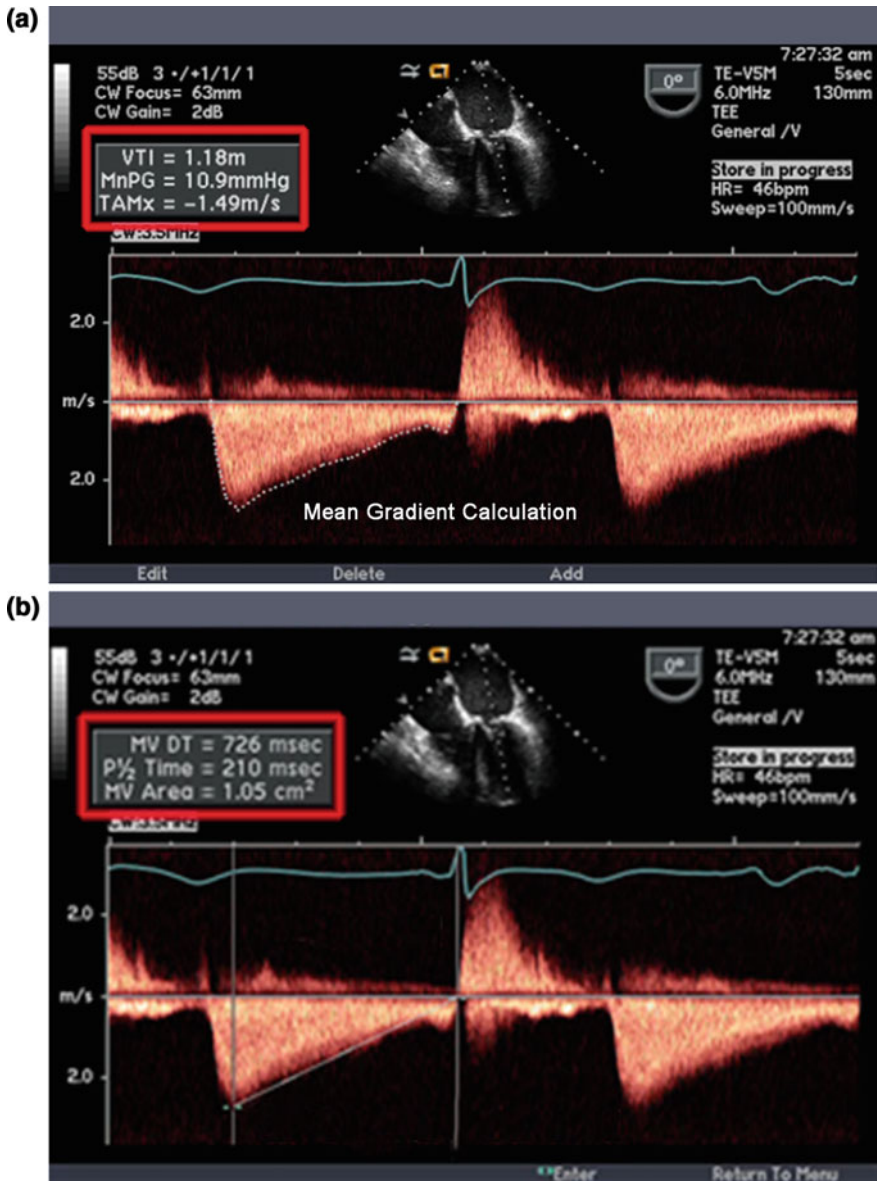

Fig. 6.13 **a** Continuous wave Doppler interrogation across the mitral valve. The mean gradient of the transmitral flow profile is calculated by tracing the entire envelope or velocity time integral. **b** The spectral Doppler profile is characterized by a high velocity E-wave with a prolonged pressure half time or deceleration time, which can be used to calculate the mitral valve area

the peak velocity of the E-wave (early filling) and drawing a caliper along the slope of deceleration, being careful to include the slope that encompasses the peak velocity and the baseline (point of zero velocity). The machine software will extrapolate the PHT in milliseconds and compute a mitral valve area. PHT measurements above 220 ms correspond to severe MS (Figs. 6.12 and 6.13a, b) [3, 24].

Proximal Isovelocity Surface Area (PISA)

Proximal isovelocity surface area (Fig. 6.14) or flow convergence method is an application of the continuity equation to measure the mitral valve area [24, 27]. As blood flow converges upon the stenotic mitral valve, a marked increase in velocity ensues, creating a series of organized hemispheres on the left atrial side of the valve. The border between blue and red on the color flow map defines the boundary between the first isovelocity hemisphere and represents the location of the first aliasing velocity, corresponding to blood traveling faster than the limit of detection (Nyquist limit) on the color flow Doppler scale. The radius of the first isovelocity hemisphere is then carefully measured along with the angle (α) that is formed by both mitral leaflets during diastole. The product of the area of the hemisphere ($2\pi r^2$) and the aliasing velocity on the color flow Doppler scale provides the volumetric flow on the atrial side. The volumetric flow on the atrial side is then multiplied by the angle correction factor, $\alpha/180°$, defined by the angle formed by the mitral leaflets, yielding a more accurate flow measurement. To calculate the mitral valve area, velocity of flow on the ventricular side must be measured by continuous wave Doppler across the mitral valve. In the ME four chamber or ME LAX view, the Doppler beam is positioned parallel to the direction of flow into the LV. The continuous wave Doppler then produces a spectral profile that can be used to

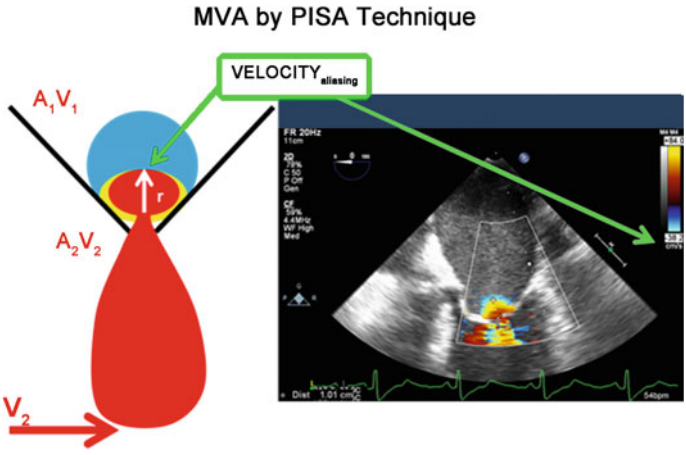

Fig. 6.14 Calculation of mitral valve area by PISA technique

calculate the maximum velocity across the valve. Using the continuity equation where the flow of blood on the atrial side equals the flow on the ventricular side

$$\text{Area}_{\text{hemisphere}} \times \text{Velocity}_{\text{aliasing}} = \text{Area}_{\text{mitral valve}} \times \text{Velocity}_{\text{mitral inflow}};$$

Mitral Valve Area can then be derived as follows:

$$\text{Area}_{\text{mitral valve}} = \alpha/180^{\circ}\left(\text{Area}_{\text{hemisphere}} \times \text{Velocity}_{\text{aliasing}}/\text{Velocity}_{\text{mitral inflow}}\right).$$

Similar to utilizing PISA for MR, using PISA for MS can be laborious and time-consuming with the potential for magnified errors in measurement of the hemisphere. Therefore measurement of PHT and mean gradients are the mainstay of estimating MS severity with PISA utilized for confirmation.

Planimetry

Planimetry is the direct measurement of the mitral valve area using two-dimensional echocardiography [24]. Trace measurement of the mitral valve area can be achieved using the transgastric basal SAX view. It is important to obtain the best image possible and utilize the freeze function on the machine to capture the valve opening in diastole. An accurate measurement of the valve area can be maximized by advancing or withdrawing the probe in attempt to move the scan plane from a superior position down to the level of the smallest valve opening. If the scan plane measures the opening above the actual orifice, the mitral valve area will be overestimated.

References

1. Silverman ME, Hurst JW. The mitral complex. Interaction of the anatomy, physiology, and pathology of the mitral annulus, mitral valve leaflets, chordae tendineae, and papillary muscles. Am Heart J. 1968;76(3):399–418.
2. Sidebotham DA, et al. Intraoperative transesophageal echocardiography for surgical repair of mitral regurgitation. J Am Soc Echocardiogr. 2014;27(4):345–66.
3. Shernan SK. Perioperative transesophageal echocardiographic evaluation of the native mitral valve. Crit Care Med. 2007;35(8 Suppl):S372–83.
4. Silbiger JJ, Bazaz R. Contemporary insights into the functional anatomy of the mitral valve. Am Heart J. 2009;158(6):887–95.
5. Mahmood F, Matyal R. A quantitative approach to the intraoperative echocardiographic assessment of the mitral valve for repair. Anesth Analg. 2015;121(1):34–58.
6. Salgo IS, et al. Effect of annular shape on leaflet curvature in reducing mitral leaflet stress. Circulation. 2002;106(6):711–7.
7. Silbiger JJ. Anatomy, mechanics, and pathophysiology of the mitral annulus. Am Heart J. 2012;164(2):163–76.

8. Mahmood F, et al. Echocardiography derived three-dimensional printing of normal and abnormal mitral annuli. Ann Card Anaesth. 2014;17(4):279–83.
9. Padala M, et al. Saddle shape of the mitral annulus reduces systolic strains on the P2 segment of the posterior mitral leaflet. Ann Thorac Surg. 2009;88(5):1499–504.
10. Hahn RT, et al. Guidelines for performing a comprehensive transesophageal echocardiographic examination: recommendations from the American Society of Echocardiography and the Society of Cardiovascular Anesthesiologists. J Am Soc Echocardiogr. 2013;26(9):921–64.
11. Lambert AS, et al. Improved evaluation of the location and mechanism of mitral valve regurgitation with a systematic transesophageal echocardiography examination. Anesth Analg. 1999;88(6):1205–12.
12. Mathew JP, et al. ASE/SCA recommendations and guidelines for continuous quality improvement in perioperative echocardiography. Anesth Analg. 2006;103(6):1416–25.
13. Silbiger JJ. Novel pathogenetic mechanisms and structural adaptations in ischemic mitral regurgitation. J Am Soc Echocardiogr. 2013;26(10):1107–17.
14. Jiang L, et al. Dynamism of the mitral annulus: a spatial and temporal analysis. J Cardiothorac Vasc Anesth. 2014;28(5):1191–7.
15. Mahmood F, et al. Changes in mitral valve annular geometry after repair: saddle-shaped versus flat annuloplasty rings. Ann Thorac Surg. 2010;90(4):1212–20.
16. Mahmood F, et al. Mitral annulus: an intraoperative echocardiographic perspective. J Cardiothorac Vasc Anesth. 2013;27(6):1355–63.
17. Mahmood F, et al. Intraoperative application of geometric three-dimensional mitral valve assessment package: a feasibility study. J Cardiothorac Vasc Anesth. 2008;22(2):292–8.
18. Owais K, et al. Three-dimensional printing of the mitral annulus using echocardiographic data: science fiction or in the operating room next door? J Cardiothorac Vasc Anesth. 2014;28 (5):1393–6.
19. Khabbaz KR, et al. Dynamic 3-dimensional echocardiographic assessment of mitral annular geometry in patients with functional mitral regurgitation. Ann Thorac Surg. 2013;95(1):105–10.
20. Lee AP, et al. Quantitative analysis of mitral valve morphology in mitral valve prolapse with real-time 3-dimensional echocardiography: importance of annular saddle shape in the pathogenesis of mitral regurgitation. Circulation. 2013;127(7):832–41.
21. Connell JM, et al. Ischemic mitral regurgitation: mechanisms, intraoperative echocardiographic evaluation, and surgical considerations. Anesthesiol Clin. 2013;31 (2):281–98.
22. Shakil O, et al. Ischemic mitral regurgitation: an intraoperative echocardiographic perspective. J Cardiothorac Vasc Anesth. 2013;27(3):573–85.
23. Shah PM. Current concepts in mitral valve prolapse–diagnosis and management. J Cardiol. 2010;56(2):125–33.
24. Wunderlich NC, Beigel R, Siegel RJ. Management of mitral stenosis using 2D and 3D echo-Doppler imaging. JACC Cardiovasc Imaging. 2013;6(11):1191–205.
25. Grayburn PA, et al. Multiplane transesophageal echocardiographic assessment of mitral regurgitation by Doppler color flow mapping of the vena contracta. Am J Cardiol. 1994;74 (9):912–7.
26. Zoghbi WA, et al. Recommendations for evaluation of the severity of native valvular regurgitation with two-dimensional and Doppler echocardiography. J Am Soc Echocardiogr. 2003;16(7):777–802.
27. Ashikhmina E, et al. Three-dimensional versus two-dimensional echocardiographic assessment of functional mitral regurgitation proximal isovelocity surface area. Anesth Analg. 2015;120(3):534–42.
28. Lambert AS. Proximal isovelocity surface area should be routinely measured in evaluating mitral regurgitation: a core review. Anesth Analg. 2007;105(4):940–3.
29. Longo M, et al. Usefulness of transesophageal echocardiography during open heart surgery of mitral stenosis. J Cardiovasc Surg (Torino). 2000;41(3):381–5.